Acoustic Coherent Backscatter Enhancement from Aggregations of Marine Animals

David R. Dowling
Department of Mechanical Engineering
University of Michigan
Ann Arbor, MI 48109-2133
phone: (734) 936-0423 fax: (734) 764-4256 email: drd@umich.edu

Award #: N00014-11-1-0258
http://www.personal.engin.umich.edu/~drd/

LONG-TERM GOALS

The overall long-term goal for this project is to determine if and how acoustic coherent backscatter enhancement (ACBE) can be used for classification of active sonar returns in a wide variety of ocean environments. During its first twenty months, this project has focused on simulations of acoustic multiple scattering from aggregations of omni-directional point scatterers to determine the parametric realms in which ACBE might be observed, and its characteristics when it is observed.

OBJECTIVES

The detailed objectives of the current research effort are to determine the parametric dependence of ACBE peak amplitude, peak emergence rate, peak angular width, and peak time dependence. Here the independent parameters are source-scatterer range, receiving array characteristics, incident wave characteristics (wave type, waveform, frequency, bandwidth, duration), and aggregation characteristics (scatterer cross section, mean spacing, resonant frequency, overall aggregation size and shape, etc.). Eventually, underwater waveguide characteristics will be considered as well.

APPROACH

The current approach involves numerical evaluation of the fundamental equations of multiple scattering from an aggregation of omni-directional point scatters[1]. If $\psi(\mathbf{r})$ is the harmonic acoustic pressure field at frequency ω at the point $\mathbf{r}$ and $\psi_0(\mathbf{r})$ is the harmonic field incident on the aggregation of scatterers located at $\mathbf{r}_n$, then

$$\psi(\mathbf{r}) = \psi_0(\mathbf{r}) + \psi_s(\mathbf{r}) = \psi_0(\mathbf{r}) + \sum_{n=1}^{N} g_n \psi_n(\mathbf{r}_n) G(\mathbf{r}, \mathbf{r}_n) \,, \tag{1}$$

where $\psi_s(\mathbf{r})$ is the scattered field and is given by the sum in (1), N is the number of scatterers, g_n is the scattering coefficient of the n^{th} scatter, $\psi_n(\mathbf{r}_n)$ is the field incident on the n^{th} scatterer,

$$\psi_n(\mathbf{r}_n) = \psi_0(\mathbf{r}_n) + \sum_{j=1, j\neq n}^{N} g_j \psi_j(\mathbf{r}_j) G(\mathbf{r}_n, \mathbf{r}_j) \tag{2}$$

and $G(\mathbf{r}_n, \mathbf{r}_j)$ is the free-space Green's function between the locations $\mathbf{r}_n$ and $\mathbf{r}_j$,

Report Documentation Page

Form Approved
OMB No. 0704-0188

1. REPORT DATE	2. REPORT TYPE	3. DATES COVERED
2012	**N/A**	**-**

4. TITLE AND SUBTITLE	5a. CONTRACT NUMBER
Acoustic Coherent Backscatter Enhancement from Aggregations of Marine Animals	5b. GRANT NUMBER
	5c. PROGRAM ELEMENT NUMBER
6. AUTHOR(S)	5d. PROJECT NUMBER
	5e. TASK NUMBER
	5f. WORK UNIT NUMBER
7. PERFORMING ORGANIZATION NAME(S) AND ADDRESS(ES) **Department of Mechanical Engineering University of Michigan Ann Arbor, MI 48109-2133**	8. PERFORMING ORGANIZATION REPORT NUMBER
9. SPONSORING/MONITORING AGENCY NAME(S) AND ADDRESS(ES)	10. SPONSOR/MONITOR'S ACRONYM(S)
	11. SPONSOR/MONITOR'S REPORT NUMBER(S)

12. DISTRIBUTION/AVAILABILITY STATEMENT
Approved for public release, distribution unlimited

13. SUPPLEMENTARY NOTES
The original document contains color images.

14. ABSTRACT

15. SUBJECT TERMS

16. SECURITY CLASSIFICATION OF:			17. LIMITATION OF ABSTRACT	18. NUMBER OF PAGES	19a. NAME OF RESPONSIBLE PERSON
a. REPORT	b. ABSTRACT	c. THIS PAGE			
unclassified	**unclassified**	**unclassified**	**SAR**	**7**	

$$G(\mathbf{r}_n,\mathbf{r}_j)=\frac{\exp\left\{-ik_0\left|\mathbf{r}_n-\mathbf{r}_j\right|\right\}}{\left|\mathbf{r}_n-\mathbf{r}_j\right|} \tag{3}$$

where $k_0 = \omega/c$ is the wave number magnitude of the incident field, c is the sound speed, and $i=\sqrt{-1}$. When the incident field and the scattering coefficients are known, equation (2) can be written N times, once for each scatterer $1 \le n \le N$, and these N algebraic equations can be solved to determine $\psi_n(\mathbf{r}_n)$. The total field at any location is then recovered from (1) using the known $\psi_0(\mathbf{r})$, the known g_n, and the calculated $\psi_n(\mathbf{r}_n)$. This formulation is akin to the direct boundary-integral formulation of computational acoustics with one computational element assigned to each scatterer. The computational burden of this approach is set by the inversion of the fully-populated N-by-N algebraic system that determines $\psi_n(\mathbf{r}_n)$.

In the current investigation, the scatterers are considered to be identical bubbles so the N scattering coefficients are all the same

$$g_n = g_1 = \left(\frac{\sigma_s}{4\pi}-\frac{k_0^2\sigma_e^2}{16\pi^2}\right)^{1/2} - i\frac{k_0\sigma_e}{4\pi}\,, \tag{4}$$

where σ_s and σ_e are the scattering and extinction cross sections, respectively. These may be determined from standard-textbook acoustic bubble formulae[2], but so far only the frequency-dependent scattering cross section σ_s has been used with $\sigma_e = \sigma_s$. For the current calculations, the incident field $\psi_0(\mathbf{r})$ is a unity amplitude plane wave with wave number vector $\vec{k}_0$, and the backscatter direction ($\theta = 0$) is defined with respect to $\vec{k}_0$ as shown in Figure 1. Spherical aggregations of scatterers have been the primary geometry considered this fiscal year.

To search for the presence or absence of ACBE, the scattered field $\psi_s(\mathbf{r})$ predicted by (1) is calculated on a far-field ring of radius R that encircles the aggregation of scatterers, with $k_o d^2/R << 1$, where d is the aggregation diameter. For simplicity, the ring, the center of the aggregation, and $\vec{k}_0$ are coplanar. For this geometry, the predicted scattered field on the ring depends on the scattering angle θ,

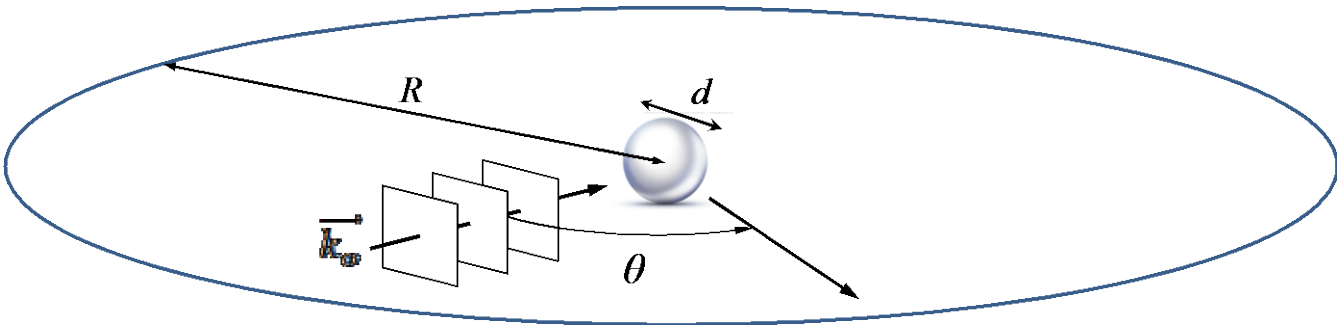

Figure 1. Geometrical configuration of the multiple scattering simulations. A plane wave with unity amplitude and wave number vector $\vec{k}_o$ impinges on a spherical aggregation of scatterers. Here d is the aggregation diameter, θ is the scattering angle (θ = 0 is the backscatter direction), and the scattered field is evaluated on a ring of radius R that encircles the aggregation.

so evidence of ACBE is determined by plotting the mean-square scattered-field ratio $\left\langle |\psi_s(R,\theta)|^2 \right\rangle \Big/ \left\langle |\psi_s(R,\theta)|^2 \right\rangle_{average}$ vs. θ, where the angle brackets indicate an ensemble average over 64 or more realizations of the random aggregation of scatterers, and the subscript "average" implies an average over scattering angle from –150° to +150°. This angle-averaging interval excludes forward scattering from the aggregation that interferes with the incident field to produce the aggregation's shadow. A peak in the mean-square scattered-field ratio centered at $\theta = 0$ indicates ACBE. Prior results from optical coherent backscattering enhancement suggest the mean-square scattered-field ratio may reach two. When the mean-square scattered-field ratio is unity at $\theta = 0$, ACBE is absent.

These ACBE investigations are the current doctoral research of Ms. Adaleena Mookerjee. She is a US Citizen and a Ph.D. candidate, and will make a presentation on this topic at the upcoming meeting of the Acoustical Society of America in Kansas City.

In addition, an undergraduate team supported by NAVSEA through the Naval Engineering Education Center (NEEC) has developed a tank experiment (42" diameter, 42" depth, 16 receiving hydrophones) that may eventually be suitable for short-range ACBE experiments in the frequency range from 30 kHz to 100 kHz.

WORK COMPLETED

Multiple-scattering simulations have been performed for spherical aggregations of as many as 1000 randomly-placed scatterers and involving as many as 4096 Monte-Carlo trials at acoustic frequencies from a factor of two below to a factor of two above a nominal bubble resonance frequency of 1.0 kHz (3.3 mm bubble radius). For the simulation results reported here, the aggregation diameter was 6 m, and a minimum scatterer separation of 0.5 m was enforced.

To investigate acoustic energy conservation, the net radial acoustic power Π in the whole field $\psi(\mathbf{r})$ from one or more scatterer realizations was computed by numerically integrating the radial intensity on a spherical surface of radius r enclosing the aggregation.

$$\Pi = \int_{\phi=0}^{2\pi} \int_{\theta=0}^{\pi} \frac{1}{2} \mathrm{Re}\left\{ -\frac{\psi^*(\mathbf{r})}{i\omega\rho} \frac{\partial \psi(\mathbf{r})}{\partial r} \right\}_{|\mathbf{r}|=r} r^2 \sin\theta \, d\theta \, d\phi \tag{5}$$

Here θ is the polar angle shown in Figure 1, ϕ is the associated azimuthal angle (not shown), and ρ is the fluid density. Ideally, Π should be zero since an aggregation of scatterers should not produce any acoustic power, and the incident plane wave should have equal power-in and power-out contributions over the surface of a sphere. Thus, (5) provides a means to assess the validity of simulation results from (1) – (4) since modeling limitations, coding mistakes, and numerical limitations – if they exist – would likely cause Π to be non-zero.

RESULTS

Sample ACBE simulation results for 1000 scatterers, 64 Monte-Carlo trials, and three frequencies near and at the bubble resonance frequency (1.0 kHz) are shown in the three panels of Figure 2. In each

case, the vertical axis is $\left\langle |\psi_s(R,\theta)|^2 \right\rangle \Big/ \left\langle |\psi_s(R,\theta)|^2 \right\rangle_{average}$ and the horizontal axis is the scattering angle θ. The central peak at $\theta = 0$ on each plot is produced by coherent backscattering enhancement. The plotted curves are terminated at ±130° to exclude the beginnings of the aggregation's shadow zone from the plots. Interestingly, all three enhancements are well above the factor of two found in prior studies involving extended scattering media. This preliminary result of greater-than-expected backscattering enhancement is surprising and unexplained at the current time.

As a first step to determine if these results are correct, the simulations were checked for acoustic energy conservation via a numerical implementation of Equation (5). For all the calculations reported here, the ratio of the numerically-determined value of Π divided by the acoustic power incident on one scatterer, $\sigma_s |\psi_0|^2 / 2\rho c$, is less than 0.005. Furthermore, the acoustic power in the backscattered peak is typically of order 10^2 times greater than the imprecision in these simulations. Thus, these simulation results may be representative of actual scattering physics for aggregations of acoustically-compact omni-directional point scatterers illuminated by a plane wave.

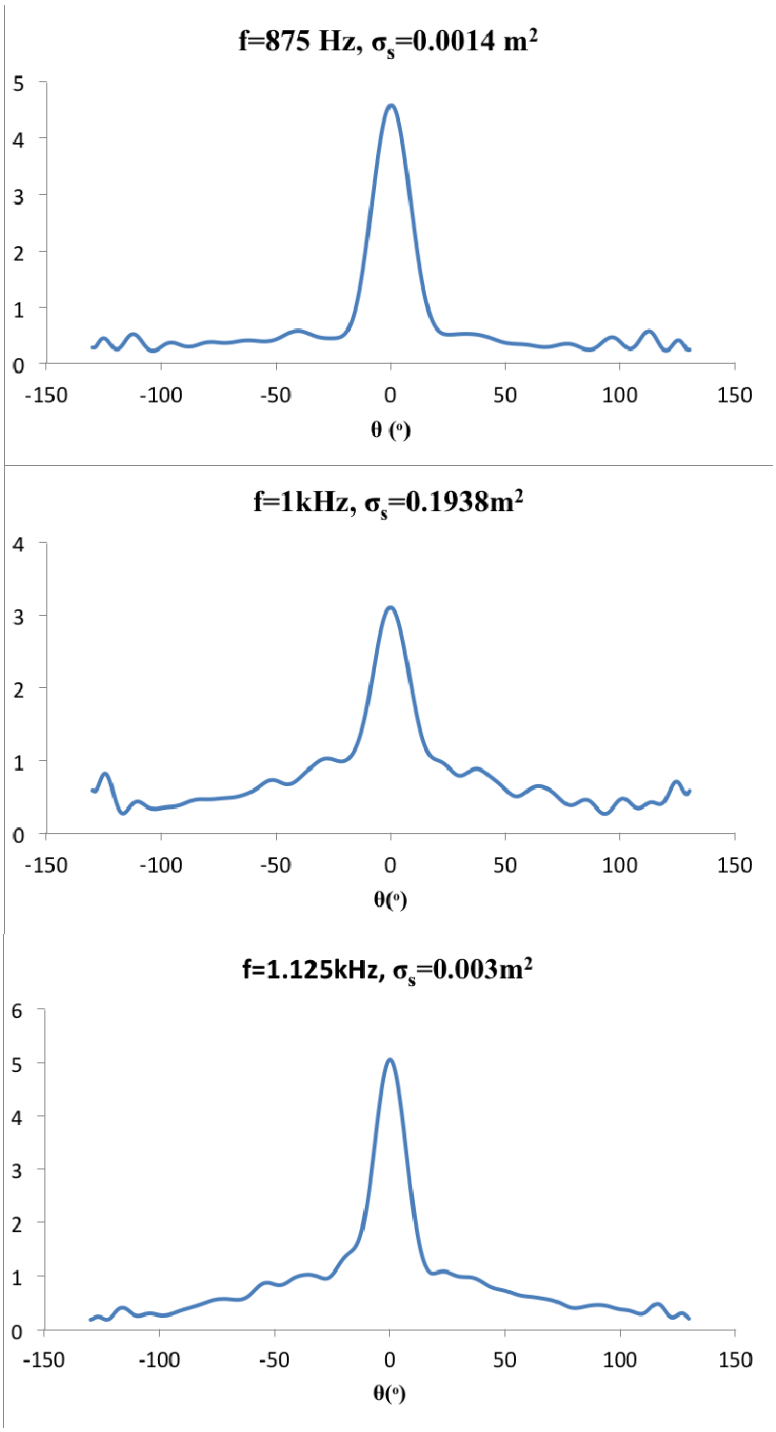

Figure 2. Mean-square scattered-field ratio $\left\langle \left|\psi_s(R,\theta)\right|^2 \right\rangle \Big/ \left\langle \left\langle \left|\psi_s(R,\theta)\right|^2 \right\rangle \right\rangle_{average}$ ***vs. scattering angle*** θ ***at three frequencies near 1.0 kHz for 1000 scatterers placed in a 6-m-diameter spherical aggregation. The ensemble average was computed from 64 Monte-Carlo trials. The scatterers are bubbles with a resonance frequency of 1.0 kHz. The acoustic coherent backscatter enhancement shown here is above that expected from prior optical and acoustic studies involving extended scattering media.***

Sample results from this investigation into acoustic energy conservation are shown in Figure 3 for a frequency of 1.0 kHz and a scatter cross section of 0.70 m^2. This cross section is near the upper limit allowed by Equation (4) when $\sigma_e = \sigma_s$, and therefore represents a strenuous test of acoustic energy conservation for the current simulations. The left panel of Figure 3 is a radial intensity map for a 20-m-radius spherical surface centered on a spherical aggregation of 1000 randomly-placed scatterers. The horizontal and vertical axes of this intensity map are the polar angle θ, varying from 0 to π, and the azimuthal angle ϕ, varying from 0 to 2π, respectively. This panel provides a colored rendition of the integrand of Equation (5) over the entire surface of the 20-m-radius sphere and includes contributions from both the incident and scattered fields. Here blue and red correspond to the acoustic energy propagating toward and away from the origin, respectively. The overall blue-to-red trend with increasing θ seen in the left panel of Figure 3 is the radial-intensity signature of the incident plane wave. The middle panel of Figure 3 is the same as the left one except it only shows the scattered-field's radial intensity. The thin non-blue vertical strip near $\theta = \pi$ is the acoustic shadow cast by the aggregation of scatterers. The right panel of Figure 3 also shows the scattered-field's radial intensity but the angular and dynamic ranges of the middle panel are reduced so that the ACBE peak is visible as the uneven vertical orange strip near $\theta = 0$. All the results shown in Figure 3 are from a single realization of the spherical aggregation.

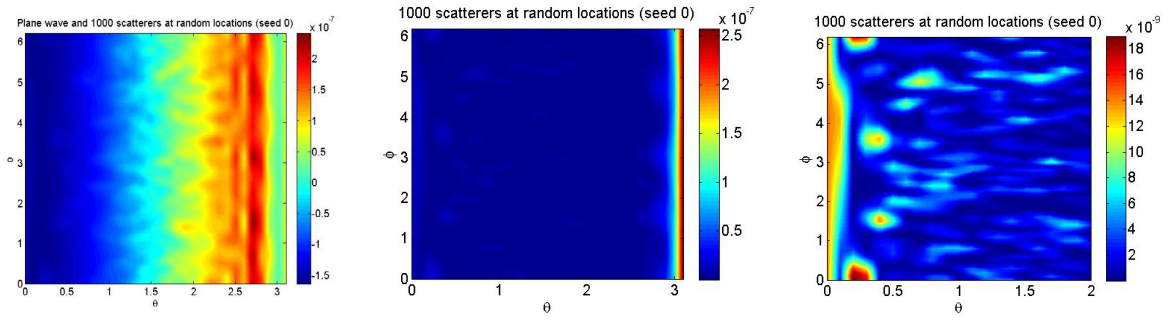

Figure 3. Radial intensity maps at a distance of 20 m for a single aggregation of 1000 scatterers randomly placed within 6-m-diameter sphere as function of the polar angle θ (see Figure 1) and the azimuthal angle ϕ. The left panel is the total radial intensity (incident and scattered), the integrand of Equation (5). The middle and right panels are the radial intensity of the scattered field alone over the full range of θ (middle panel), and a reduced range of θ (right panel) that emphasizes the backscatter direction. The red strip on the right side of the middle panel is the acoustic shadow of the aggregation. The uneven orange strip on the left side of the right panel is the acoustic coherent backscatterer enhancement peak.

If these new and unexpected results survive a variety of other simulation tests, a journal article covering these results will likely be submitted by end of the calendar year.

IMPACT/APPLICATION

In broad terms, this project ultimately seeks to determine if and how ACBE might be exploited for active sonar applications. In particular, if successful, it should prove useful for remote classification, because a large sonar return from a single large scatter will likely not display ACBE while a similarly large sonar return from an aggregation of many small scatterers may display ACBE. Thus, this research effort may eventually impact how active sonar signals are processed and displayed for tactical decision-making related to classification.

TRANSITIONS

The results of this research effort should aid in the design of active sonar signal processors for tactical decision aids. However, at this time no direct transition links have been established with more applied research programs. Once the current simulation capability is more firmly established and validated, and promising results have been obtained, a transition path through NRL or one of the Navy's Warfare Centers will be sought.

RELATED PROJECTS

This project is related the other projects funded under ONR's 2010 basic research challenge program. In particular, the work by Prof. Feuillade in Chile is most closely related.

REFERENCES AND PUBLICATIONS

[1] Foldy, L.L. (1945) "The multiple scattering of waves, I. General theory of isotropic scattering by randomly distributed scatterers," Physical Review Vol. 67, 107-119.

[2] Kinsler et al. (2000) "Fundamentals of Acoustics," Wiley, New York, pp. 238-241.

[3] Akkermans, E., Wolf, P.E., and Maynard, R. (1986) "Coherent backscattering of light by disordered media: analysis of the peak line shape," *Physical Review Letters*, Vol. 56, No. 14, 1471-1474.